5

Temperature

Although many methods exist with which to determine temperatures of liquids and solids, the measurement of air temperature is complicated by the poor thermal conductivity of still air and the presence, during the day, of solar radiation which directly heats thermometers. Consequently, air temperature measurement depends not only on the thermometer employed, but on its exposure. In particular, the uncertainty resulting from solar radiation heating up a thermometer is known as the *radiation error* (see Section 5.5), which causes a thermometer to become warmer than the air to which it is exposed. This effect can cause large uncertainties, and is present in almost all daytime surface and airborne temperature measurements. Thermometer exposure is therefore an important aspect of air temperature measurement in general, requiring a combination of shade, protection from precipitation and good ventilation (see Section 5.5.2). Two methods of thermometry operating on different principles which do not require efficient conduction between the air and the sensor are acoustic thermometry (see Section 8.2.6) and infrared thermometry (see Section 9.7.5).

Temperature difference determines the direction of heat flow between two bodies in thermal contact. There is no heat flow between two bodies if they are in thermal equilibrium, when their temperatures will be equal. Measurement of temperature depends on the existence of thermometric properties of substances, such as the expansion of solids or liquids with temperature or a change in resistance. Many physical properties of solids provide such a thermal response, however, the abundance of different thermometric properties can also complicate a temperature measurement, if other temperature-dependent changes occur in addition to the primary thermometric property sought. An example would be a device using resistance as its primary thermometric property, in which both the sensing element *and* the connecting wires showed a change in resistance with temperature. These and similar errors can usually be reduced or eliminated by good experimental technique.

5.1 The Celsius temperature scale

The standard international temperature scale is based on properties of an ideal gas, leading to the thermodynamic temperature scale. The thermodynamic (Kelvin) scale uses the triple point[1] of

water as a fixed point, with the divisions of the scale made equal to (1/273.16) of this temperature. Each of these divisions is known as 1 K.

Temperatures measured in Kelvin are needed in evaluating thermodynamic properties of atmospheric gases, but for surface air temperature measurements, the Celsius scale often becomes more practical. The Celsius scale shifts the thermodynamic scale by a fixed offset, so that a temperature T_K (in Kelvin) is given as T_C (in Celsius) by

$$T_C = T_K - 273.15\,. \tag{5.1}$$

Because there is only an offset between T_C and T_K, the size of the temperature unit is the same in Kelvin and Celsius. Using the Celsius scale, the triple point of water is 0.01°C, the melting point of ice and boiling point of water are about 0°C and 100°C respectively depending on the pressure, and absolute zero (0 K) is −273.15°C.

5.2 Liquid in glass thermometry

5.2.1 Fixed interval temperature scales

Early temperature scales used the melting and freezing points of convenient materials to define temperature scales empirically, for a particular thermometer (see also Section 1.4). To determine temperatures lying between these fixed points, the thermometer's scale was divided equally. Such an empirical temperature scale is necessarily specific to the thermometer in use, because of non-linearity in the thermometric property employed. Hence comparison between temperatures measured on two empirical scales using the same fixed points but different thermometric properties is difficult if high precision is required.

An important empirical temperature scale is the Centigrade scale. This employs one hundred equal divisions between two assigned temperatures, assuming that the thermometric property employed is linear. Therefore, if the thermometric property has some value X which lies between the lower fixed point X_0 and upper fixed point X_{100}, the temperature associated with the value X will be

$$\theta(X) = 100\frac{(X - X_0)}{(X_{100} - X_0)}\,. \tag{5.2}$$

If the lower and upper fixed points are (as is usual) the melting point of ice[2] and the boiling point of water respectively, at one atmosphere pressure, the Centigrade and Celsius scales will, despite

their fundamentally different origins, show approximate numerical agreement if non-linearity in the thermometric properties is small.

5.2.2 Liquid-in-glass thermometers

The fixed interval temperature scale is closely associated with the liquid-in-glass (LiG) thermometer which is still widely used for general-purpose measurements in air or liquids. A LiG thermometer uses thermal expansion of a liquid as its thermometric property, with alcohol or mercury the liquid commonly used in thermometers for atmospheric applications. The cubic thermal expansivity of a liquid α is the fractional change in the liquid's volume for a unit change in temperature. For a volume of liquid V_0 at a temperature T_0, the change in volume ΔV when the temperature has changed to T is given by

$$\Delta V = \alpha V_0 (T - T_0)\,. \tag{5.3}$$

If the liquid is constrained within the glass tube of the thermometer, its expansion can be measured from a scale ruled on the glass (Figure 5.1).

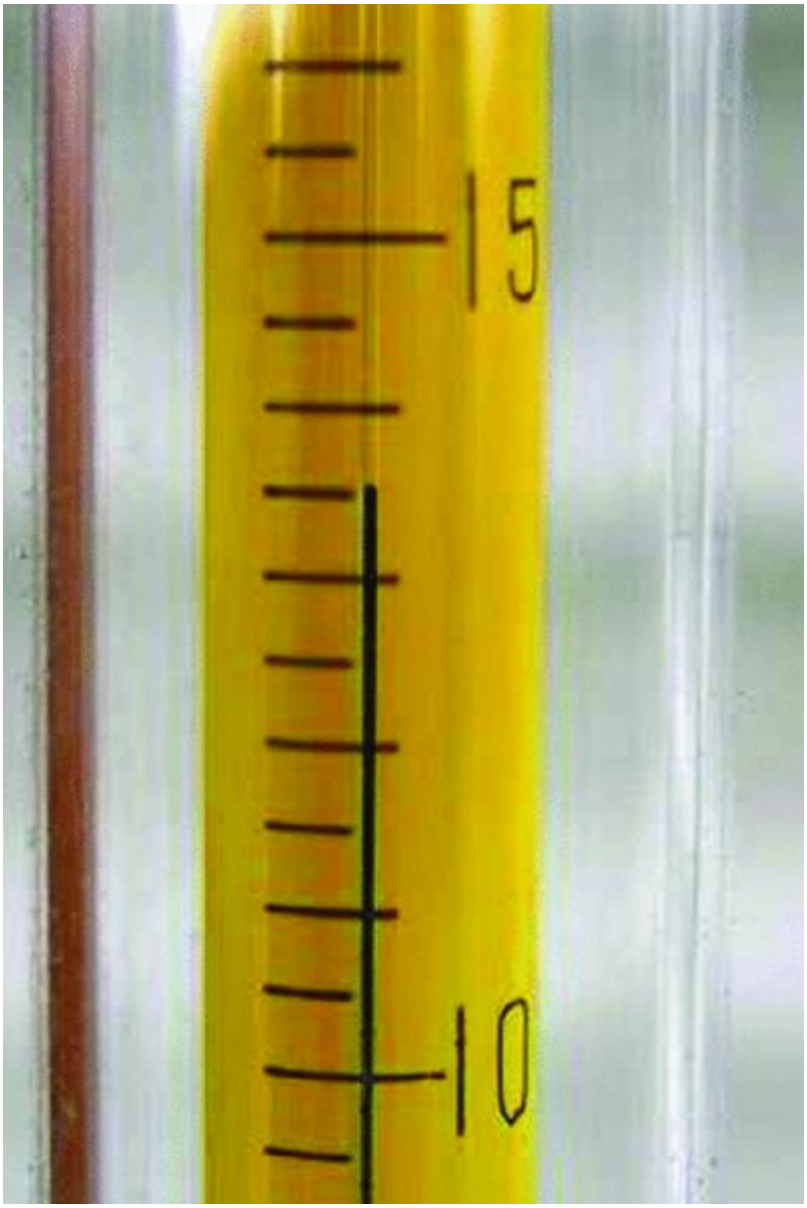

Figure 5.1 The scale engraved on the outer surface of a liquid-in-glass mercury thermometer. This type of thermometer can be read to ± 0.1°C (in this case it is indicating 13.5°C), but whether this is justified depends on its calibration.

A LiG thermometer typically has a cylindrical geometry, that is, the expansion or contraction of the liquid occurs along a glass bore of constant circular cross section. For a bore of radius r, the sensitivity of the thermometer (the change in length of the liquid thread per unit change in temperature) is

$$\frac{\Delta l}{\Delta T} = \frac{\alpha V_0}{\pi r^2}, \tag{5.4}$$

where V_0 is the volume of liquid contained at a reference temperature T_0. A sensitive thermometer therefore requires thin bore glass tubes and/or a large reservoir of liquid in the

sensing bulb. To encompass a wide range of temperatures, the stem may need to be long. In variants of LiG thermometers used for soil temperature measurements, the sensing bulb is manufactured to be at right angles to the scale, allowing the thermometer to be read without removing it from the soil.

Alcohol and mercury are commonly used for thermometry, and their properties are summarised in Table 5.1. Although alcohol has the larger expansivity, mercury is preferred as it provides a well-defined meniscus, and does not adhere to the glass of the thermometer body. Mercury is also opaque, whereas alcohol has to have a dye added to provide contrast with the glass body of a thermometer. A practical disadvantage of mercury (other than its toxicity) arises because it freezes at −39°C. Alcohol thermometers consequently have to be used for LiG temperature measurements below this temperature, and for minimum thermometers.[3] These can show poorer long-term stability than mercury thermometers.

Table 5.1 Properties of liquids used in thermometry

Liquid	Cubic expansivity (10^{-3} K^{-1})	Melting point
Alcohol	1.12	−114°C
Mercury	0.81	−39°C
Water	0.21	0°C

Accuracy of LiG thermometers is typically ±0.2°C, even though their resolution may be better, for example, with 0.1°C divisions. The typical exponential response time is 30 s, so about 100 s is needed to give a steady reading (see Section 2.2.1). This time scale depends on the size of the sensing bulb, which, as well as influencing the sensitivity, determines the thermal capacity of the device. Some sources of uncertainty specific to LiG thermometers are given in Table 5.2.

Table 5.2 Summary of uncertainties associated with liquid-in-glass thermometers

Aspect	Comment
Scale errors	Arise from a combination of non-linear expansion of the liquid or non-uniformity in the bore; minimised by calibration.
Thread errors	Breaks occurring in liquid thread, which may arise in alcohol thermometers.
Emergent stem error	During calibration, a thermometer may have its bulb immersed in a fluid but with its stem emerging, leading to a temperature gradient along the glass of the thermometer.
Parallax errors	Arise from refraction within the glass; observer's eye level should be at the same level as the liquid level.
Radiation errors	Reduced by using radiation shields, such as polished metal, and by ventilating the sensor (see Section 5.5).

5.3 Electrical temperature sensors

Electrical thermometers of different kinds present a range of alternative technologies to the LiG thermometers, through providing a voltage (e.g. a thermocouple or semiconductor thermometer) or resistance (e.g. a thermistor or metal resistance thermometer) output which varies with temperature.

5.3.1 Thermocouple

A thermocouple junction results when two different metals are welded, twisted or soldered together. If two such thermocouple junctions are electrically connected in series, a small emf is generated[4] which varies with the temperature difference between the two junctions (Figure 5.2).

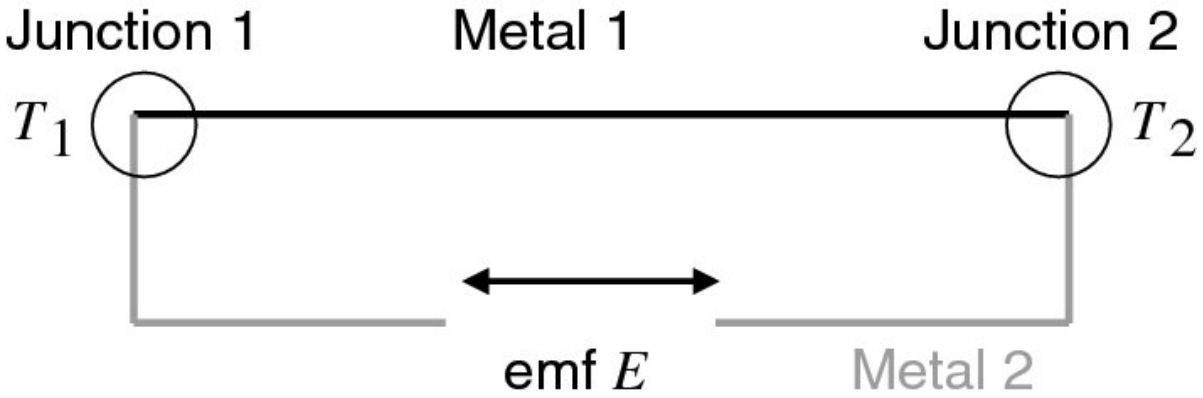

Figure 5.2 A thermocouple, constructed by making junctions 1 and 2 between two dissimilar metals. The emf generated E is proportional to the temperature difference ($T_1 - T_2$) between the two junctions.

The choice of metals (or alloys) used determines the emf generated. Common combinations of metals used for thermocouples include copper–constantan (known as 'type T' thermocouples) chromel–alumel ('type K') and iron–constantan ('type J'), which all give emfs of about 40 μV K^{-1}. The temperature-voltage characteristic of a thermocouple over a large range is non-linear, in which case it is desirable to operate at the temperature around which it is most sensitive. A thermocouple thermometer can be made physically small, requiring no more than a short section of the dissimilar wire in contact (Figure 5.3).

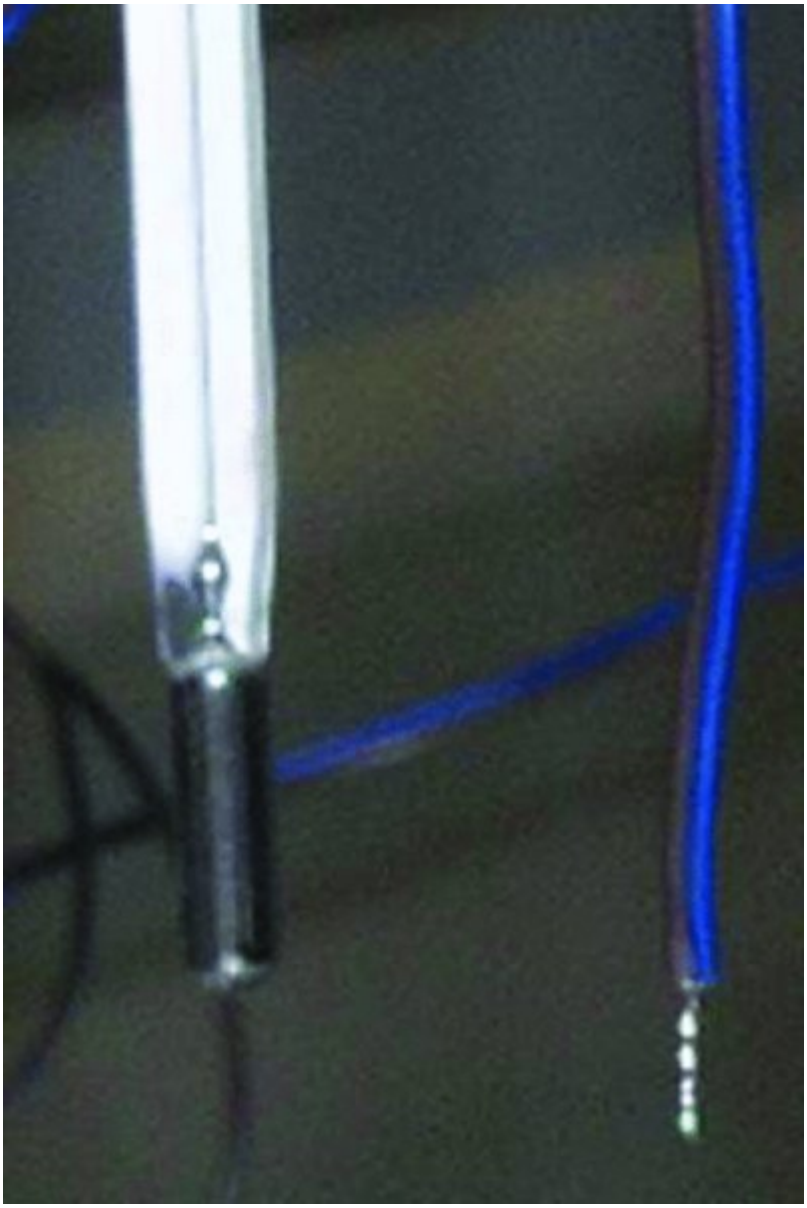

Figure 5.3 A simple thermocouple junction, constructed from two dissimilar wires twisted together.

Thermocouple junctions are usually connected differentially in pairs, with one kept at a fixed reference temperature (usually 0°C), or an electronic reference junction used to provide a fixed voltage. Thermocouples are therefore ideally suited to determining temperature differences**,** by exposing the two junctions to two different temperatures. The response time depends on mass and ventilation speed and is typically 0.5 s to 5 s. A major limitation is that the small emf produced requires a sensitive voltmeter; for example, a voltmeter reading to 1 μV is required to give a resolution of 0.025°C for a type K thermocouple. Long, or unscreened connection leads can generate noise voltages comparable with the thermocouple voltage, compromising the

measurement (see also Section 3.3). Individual thermocouples can, however, be connected in series to form a thermopile, which, as a system gives a larger output and is more sensitive than a single thermocouple, but may be physically larger.

5.3.2 Semiconductor

Many modern semiconductor temperature sensors are available, based on the variation of forward voltage across a semiconductor *pn* junction, such as that of a diode. A simple silicon diode junction has a change in forward voltage (Figure 5.4) with temperature of ~ -2 mV K^{-1}, which forms the basis for many integrated semiconductor temperature sensors.

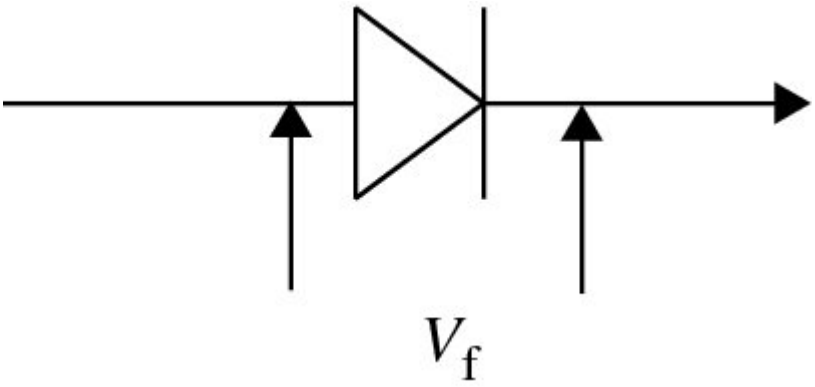

Figure 5.4 Electronic circuit symbol for a diode (anode connection on left, cathode connection on right), showing the forward voltage (V_f), which is developed across the device when a current flows through it in the direction of the arrow head.

As amplification circuitry can also be fabricated on the same semiconductor chip, amplification to give convenient linear sensitivities can be implemented, such as to generate a change of 10 mV K^{-1} for easy use with a digital voltmeter. Some semiconductor temperature devices also include analogue to digital converters, to provide a digital output directly. Using serial data transfer (one data bit sent after another, at a prearranged rate), it is possible for the sensor to need no more than three connections, two for power and one to provide the data.

Accuracy of semiconductor temperature sensors can be to about ±1°C or better without further calibration. Because of their insulating packaging material, semiconductor temperature sensors have response times which are somewhat longer than those of thermistors.

5.3.3 Thermistor

A thermistor is a semiconductor device specifically fabricated so that its electrical resistance varies markedly with temperature. Thermistors may have a positive or, more commonly, a

negative temperature coefficient.[5] A thermistor with a negative temperature coefficient can have its resistance characteristic represented by

$$R(T) = a \exp\left(\frac{b}{T}\right), \tag{5.5}$$

where R is the resistance of the device at a temperature T in Kelvin, and a and b are constants for a given material. (b is sometimes known as the characteristic temperature). The exponential dependence of resistance on temperature means that, over some ranges of temperature, a thermistor can be very sensitive i.e. its resistance changes rapidly per unit change in temperature. Thermistor resistances are usually sufficiently large to be easily measured on a simple ohmmeter, but the scale response will be non-linear.

Thermistors require standardisation to determine the constants a and b, but if the thermistors are manufactured to sufficiently close tolerances, their constants can be assumed from data sheets without a separate calibration experiment. In common with other sensors, they may need ventilation and radiation shields for use in air, but they can be made physically small. The response time depends on their mass and the ventilation speed used. It is typically 1 s to 10 s, with typical resolutions of 0.02°C. For long-term use, a thermistor has to be aged: this process ensures that any initial changes in a thermistor occur before it is put into service.

An example of the use of an ultra-miniature thermistor for temperature measurement within a water droplet is shown in Figure 5.5. The thermistor provides the mounting for the droplet, whilst measuring its temperature during supercooling. (In the original experiment [42], a heating current was applied to the thermistor after freezing had occurred, to initiate melting.) Figure 5.6 shows the variation of the droplet temperature during a cooling cycle.

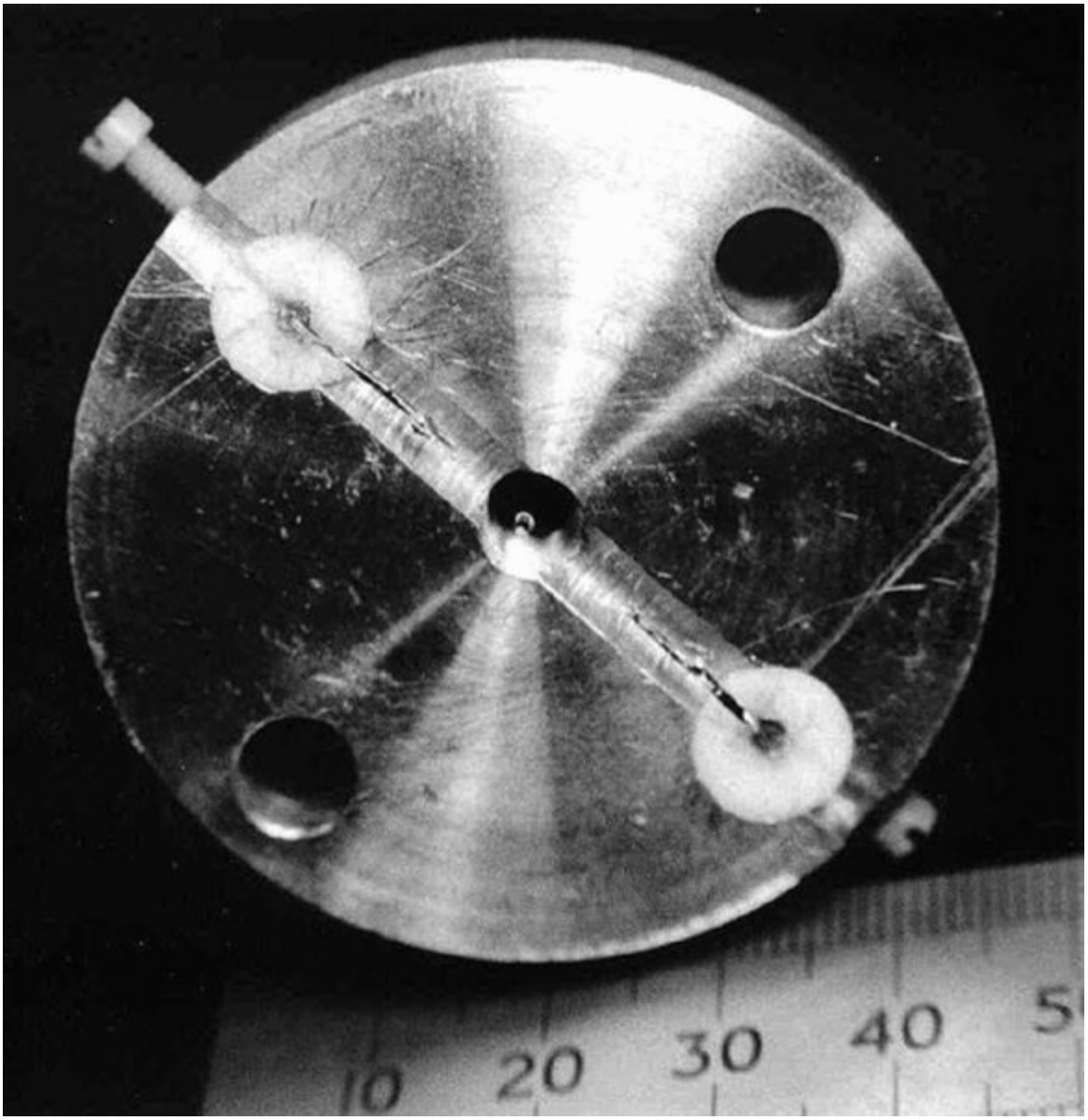

Figure 5.5 Droplet cooling apparatus using an ultra-miniature glass bead thermistor to both support and monitor a water droplet. The complete aluminium cooling chamber has been dismantled to expose the position and mounting of the water droplet on the upper aluminium block of a cooling chamber. A droplet is in the centre of the picture, held on the bead thermistor strung on its fine axial connection wires between the thick connection wires emerging from PTFE slugs. (In use, the thermistor was covered by a lower aluminium block, spaced from the thermistor and cooled by a Peltier device.)

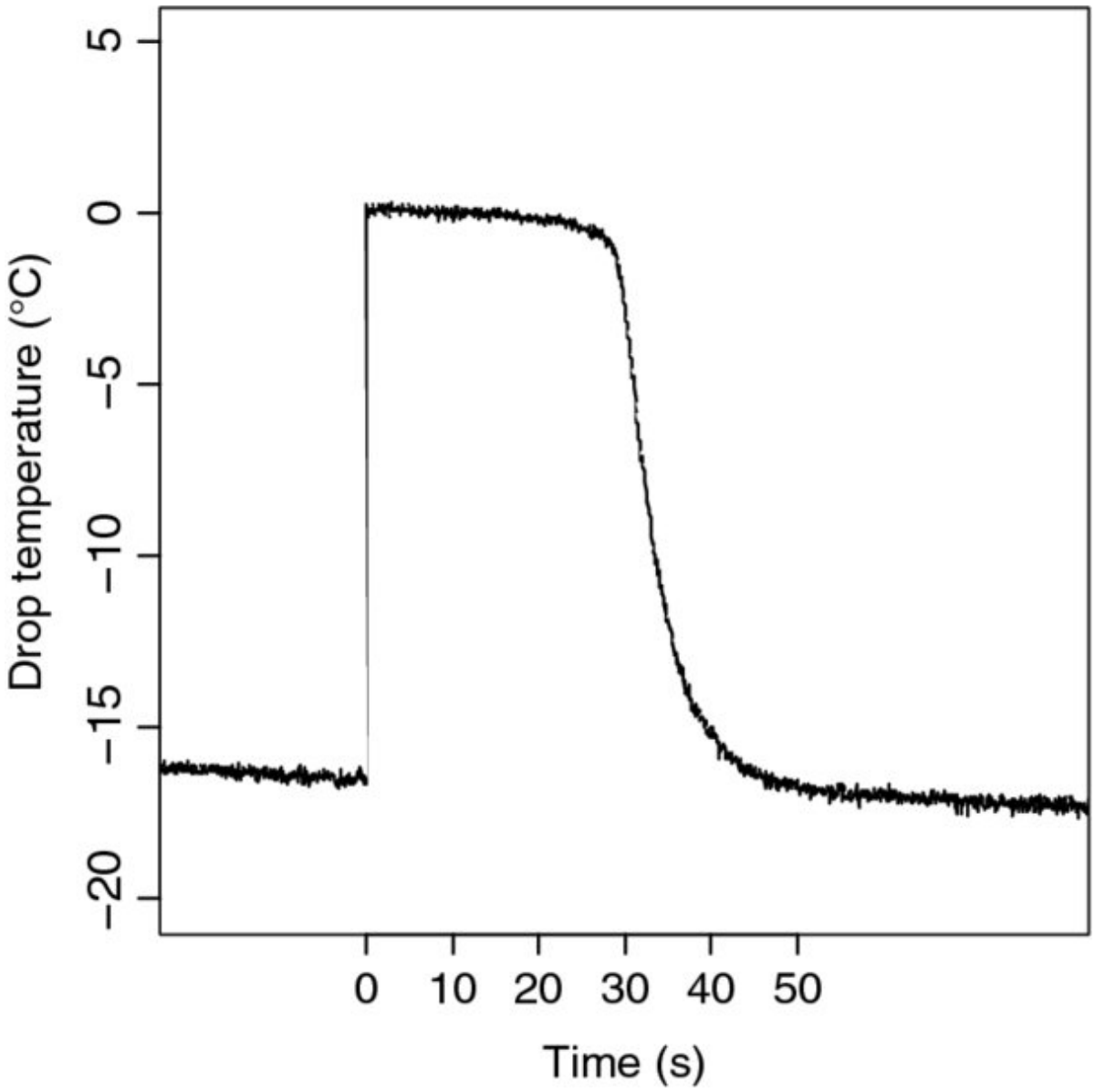

Figure 5.6 Temperature within a 1 μL water droplet, as the surrounding environment was steadily cooled. The droplet remains liquid (i.e. it supercools) until spontaneously freezing (at time = 0 s), during which its temperature instantaneously rises to about 0°C as latent heat is released. After the droplet has completely frozen, it cools to the temperature of its surroundings, at a rate proportional to the difference between its temperature and that of its surroundings. (Temperature measurements made at 12 Hz.)

5.3.4 Metal resistance thermometry

Resistance thermometry depends on the property shown by metals of an increase in resistance with temperature. As platinum has a well-defined (and substantially linear) relationship between resistance and temperature and is chemically stable, it is well suited to thermometry. The metal resistance sensing element of a Platinum Resistance Thermometer (PRT) can be engineered into a

form suitable for the intended application: high-quality resistance thermometers use a coil of platinum wire (which is stable and resistant to corrosion) in a metal case, and cheaper versions use a platinum film deposited on a ceramic substrate.

The general form of the temperature-resistance characteristic[6] is

$$R(T) = R_0 \left[1 + \alpha(T - T_0) + \beta(T - T_0)^2\right], \tag{5.6}$$

where R_0 is the resistance at a temperature T_0, and α and β are measured temperature coefficients for the metal concerned. For accurate work, the quadratic term $\beta(T - T_0)^2$ is required, but in many cases, using platinum this can be neglected as the term is small ($\beta \sim -5 \times 10^{-7}$ K^{-2}). Widely-used commercial PRTs conform to the industrial 'Pt100' standard, having a resistance of 100.0 Ω at 0°C with a temperature coefficient α of 0.00385 K^{-1}, and good long term stability without further standardisation. Their response time depends on the size and mass of the case, but is typically 30 s to 120 s. The typical temperature resolution is 0.02°C, with 0.05–0.2°C accuracy possible if used carefully. A commercial PRT sensor is shown in Figure 5.7.

Figure 5.7 Platinum resistance thermometer (resistance element enclosed within a stainless steel sheath, 8 mm diameter), used to measure the temperature of a concrete surface. (In use, a half-cylinder radiation shield is fitted into the clips.)

For air temperature measurements, a cylindrical PRT sensor would usually be used with a radiation shield of some form. However, because platinum can be made into fine wire, it is also possible instead to construct fine wire PRTs which present a much reduced area for the interception of solar radiation and small thermal inertia allowing rapid time response. Such a fine wire sensor [43] was used on the Huygens probe which landed on Saturn's moon Titan in 2005. In versions for terrestrial micrometeorology, there are similar objectives of small radiation errors and rapid time response. With fine wire sensors, it is also important to limit the signal conditioning circuitry's measurement current which passes through the fine wire sensor, to minimise errors from self-heating.

Figure 5.8 shows a fine wire platinum resistance thermometer (FWPRT) element, constructed from platinum wire wound on a plastic former. Connections for the resistance measurement are made to each end of the fine wire by a soldered joint, and additional connections are made to allow for compensation of the connection resistances. Figure 5.9 shows the same design of FWPRT used in atmospheric conditions, mounted in an array for comparison between the

sensors. Rapid fluctuations in temperature can be obtained with such sensors, as the exponential time response is ∼40 ms. The time response capability of a fine wire device for rapid changes in temperature is apparent in the measurements presented in Figure 5.10. Such thermometers are useful for studying turbulence, and for measuring the transfer of heat by turbulence (see Section 12.1.2).

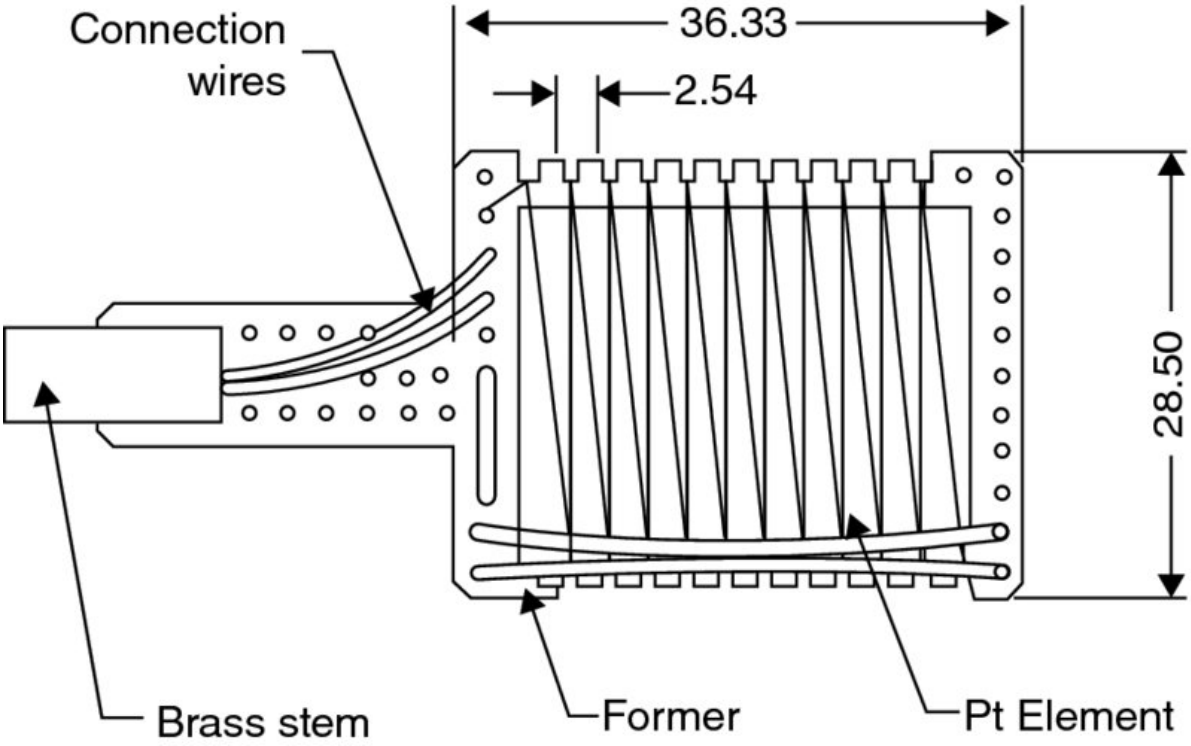

Figure 5.8 Construction of a fine wire platinum resistance thermometer, using fine (25 μm diameter) platinum wire [37] (dimensions given in millimetres).

Figure 5.9 Array of fine wire resistance thermometers arranged for an air temperature comparison. The signal conditioning electronics is mounted in the box at the base of the thermometer. This minimises the effect of connection resistances, but still requires good thermal stability of the electronics.

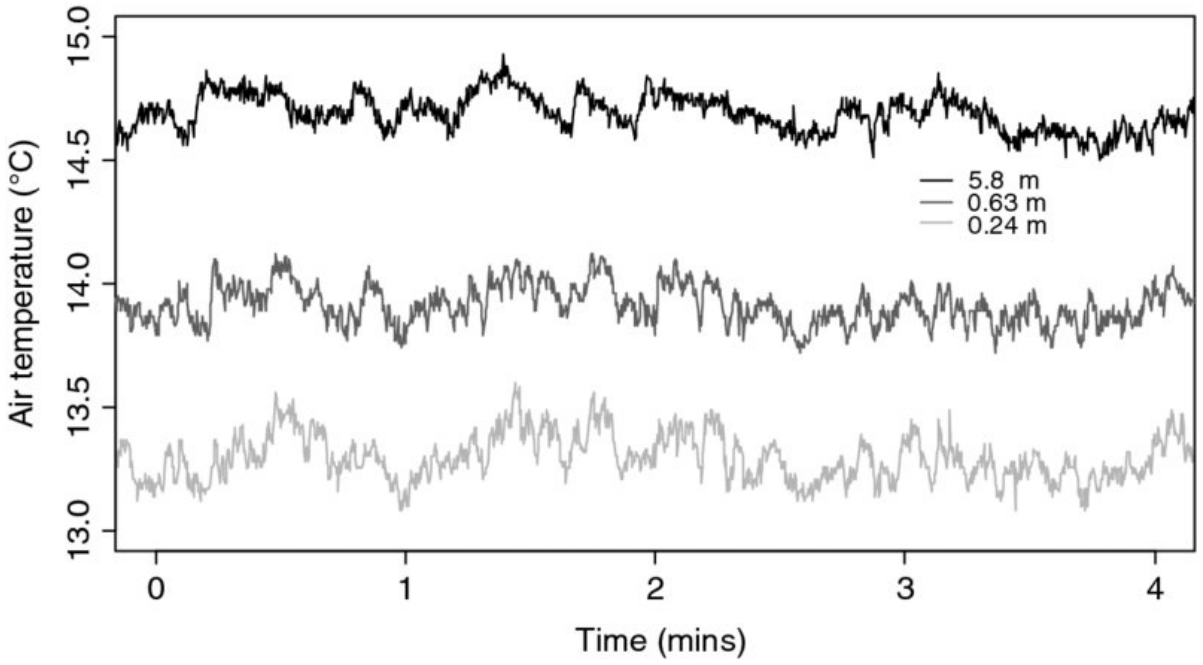

Figure 5.10 Air temperature measurements obtained over flat terrain (Camborne Met Office, Kehelland, 11 August 1999), using fine wire platinum resistance thermometers in a vertical array at 0.24 m, 0.63 m and 5.88 m above the surface.

5.4 Resistance thermometry considerations

For continuous logging of temperatures, a voltage rather than a resistance measurement will be needed. Resistance to voltage conversion is, in principle, a straightforward process but, as mentioned in Section 3.5, the accuracy of a resistance measurement depends on the magnitude of the resistance to be measured in comparison with connection resistances. The linearity of the sensor can also be a consideration, if the measurement resolution is required to be consistent across the entire measure- ment range.

5.4.1 Thermistor measurement

A key practical advantage of thermistors is that their resistances are large compared with the connection cables required, which means that they are well suited to temperature monitoring remote from the signal conditioning circuitry. However, because of their exponential response, some linearisation is desirable. The non-linear response to resistance seen in the Figure 3.19 resistance measuring circuit can be used to approximately compensate for the thermistor's exponential response. For a thermistor with a negative temperature coefficient (ntc), connecting the thermistor in the upper part of the potential divider with the resistor in the lower part (Figure 5.11) will cause the output voltage to increase with increasing temperature.

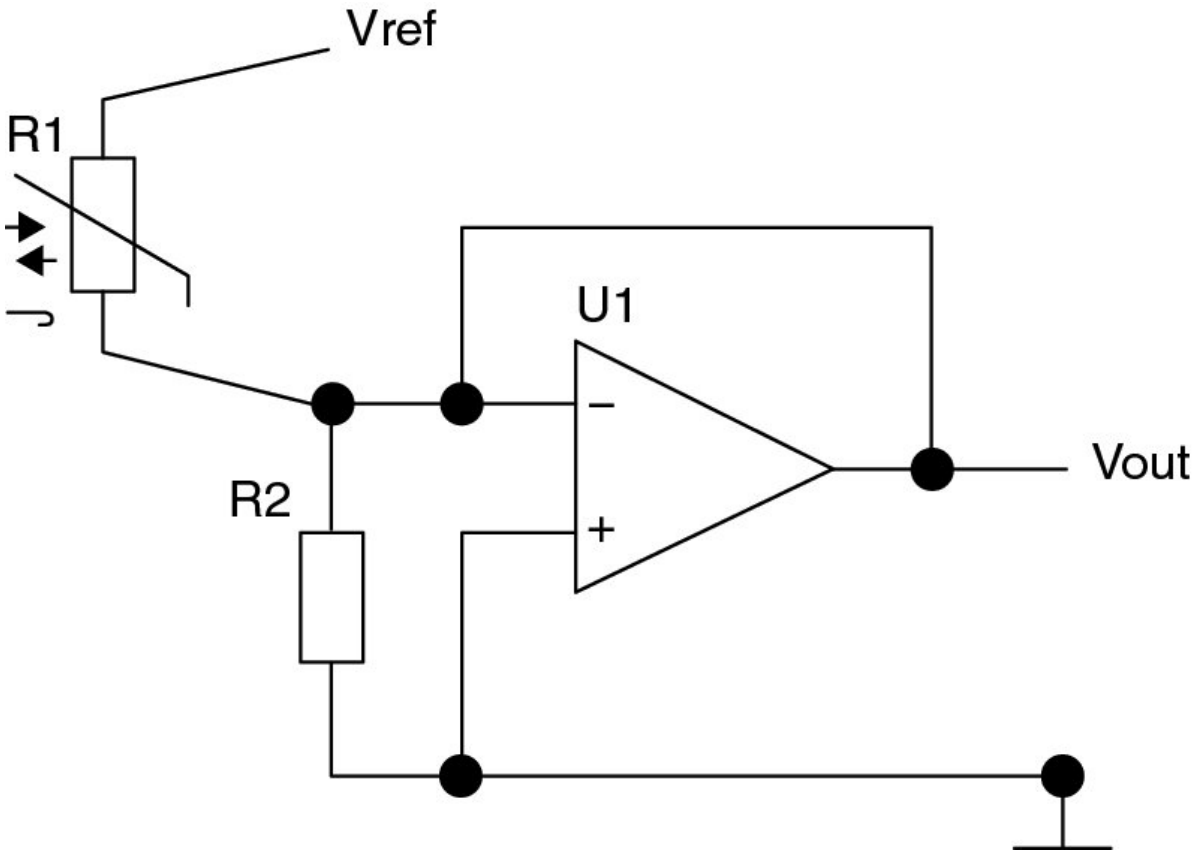

Figure 5.11 Measurement of a thermistor resistance R1 with negative temperature coefficient, using a fixed reference voltage V_{ref} and a fixed reference resistor R2. (U1 is an integrated circuit unit gain buffer stage.)

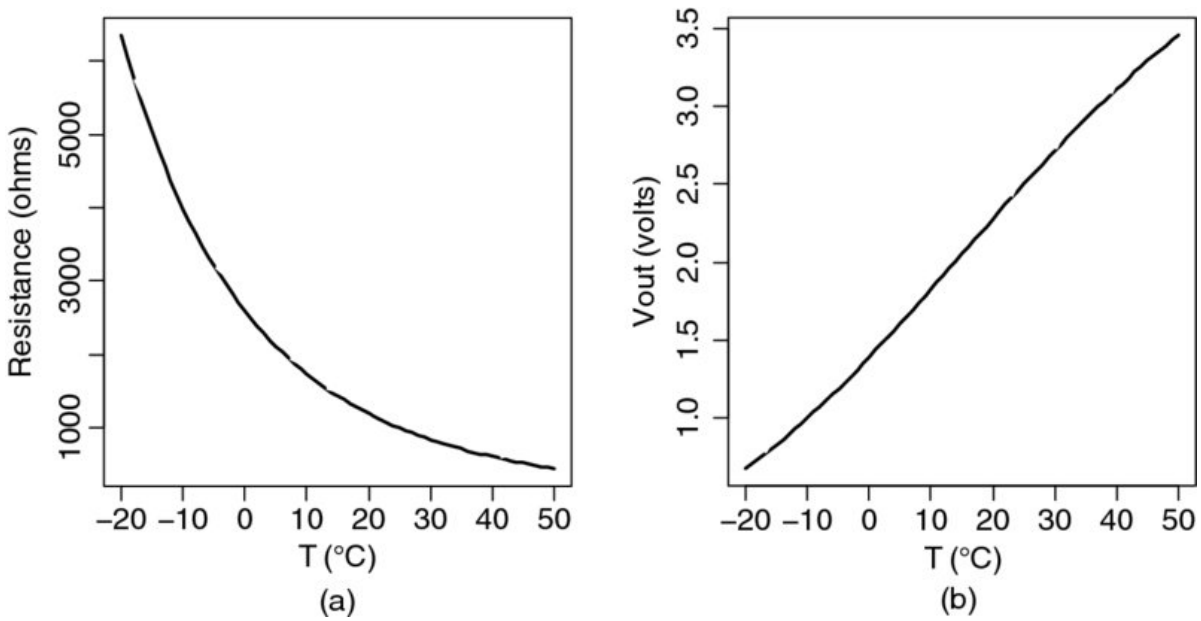

Figure 5.12 (a) Calculated resistance variation with temperature T for a negative temperature coefficient thermistor having a resistance of 1 kΩ at 298 K. (b) Calculated output voltage variation with temperature for the thermistor in (a) in the non-linear resistance measuring circuit of Figure 5.11, for R2 = 1 kΩ and V_{ref} = 5.0 V.

The full theoretical voltage-temperature response can be found by combining the thermistor characteristic (Equation 5.5) with that for the potential divider circuit (Equation 3.10), as

$$v_o = V_{\text{ref}} \frac{R}{a \exp\left(\frac{b}{T}\right) + R}, \tag{5.7}$$

where R is the fixed series resistance (R2 in Figure 5.11), V_{ref} the reference voltage and a and b the thermistor coefficients. The change in the output resistance with temperature for a typical ntc thermistor can be seen in Figure 5.12a. From Equation 5.7, the variation in output voltage v_0 with temperature is given by

$$\frac{dv_o}{dT} = V_{\text{ref}} \frac{Rab \exp\left(\frac{b}{T}\right)}{T^2 \left[a \exp\left(\frac{b}{T}\right) + R\right]^2}. \tag{5.8}$$

By optimising the choice of R, the variation with temperature of the temperature response dv_0/dT can be reduced [44]. For R about equal to the thermistor resistance in the middle of the temperature measurement range sought, the voltage-temperature characteristic of the circuit differs from a linear response by less than 1°C between −15° and 40°C (see Figure 5.12b).

5.4.2 Platinum resistance measurement

In contrast to typical thermistors, the resistance change with temperature for Pt100 sensors is highly linear through the atmospheric range of temperatures encountered, but only small (e.g. a 0.385 Ω change in resistance for each 1 K temperature change). Care must therefore be taken to allow for finite connection resistances if the sensor is remote from the signal conditioning electronics. An additional consideration is self-heating of the sensor from the measurement current, which must be minimised.

Figure 5.13 shows a practical resistance-to-voltage converter [45], using the Kelvin connection method (see Section 3.5.2) for a Pt100-like sensor whose resistance varies around a base resistance of 100 Ω at 0°C. An accurate 5 V voltage source supplies a fixed excitation current of about 50 μA through R1, R2 and the sensor resistance R, although, as (R2+R) ≪ R1, R and R2 contribute little to determining the excitation current. The excitation current develops a fixed voltage across R_2, which is amplified by a factor of 100 by a precision microvolt differential stage

(IC4). A further microvolt differential stage (IC5) amplifies the voltage generated across the sensor resistance, which will vary with temperature, by the same amount. The difference between the outputs of IC4 and IC5 is determined by differential amplifier IC6a, which will vary with *R*. Further amplification is provided by IC6b to ensure the output goes positive with increasing resistance, with the gain chosen to give an output voltage change suitable for the resistance change envisaged.

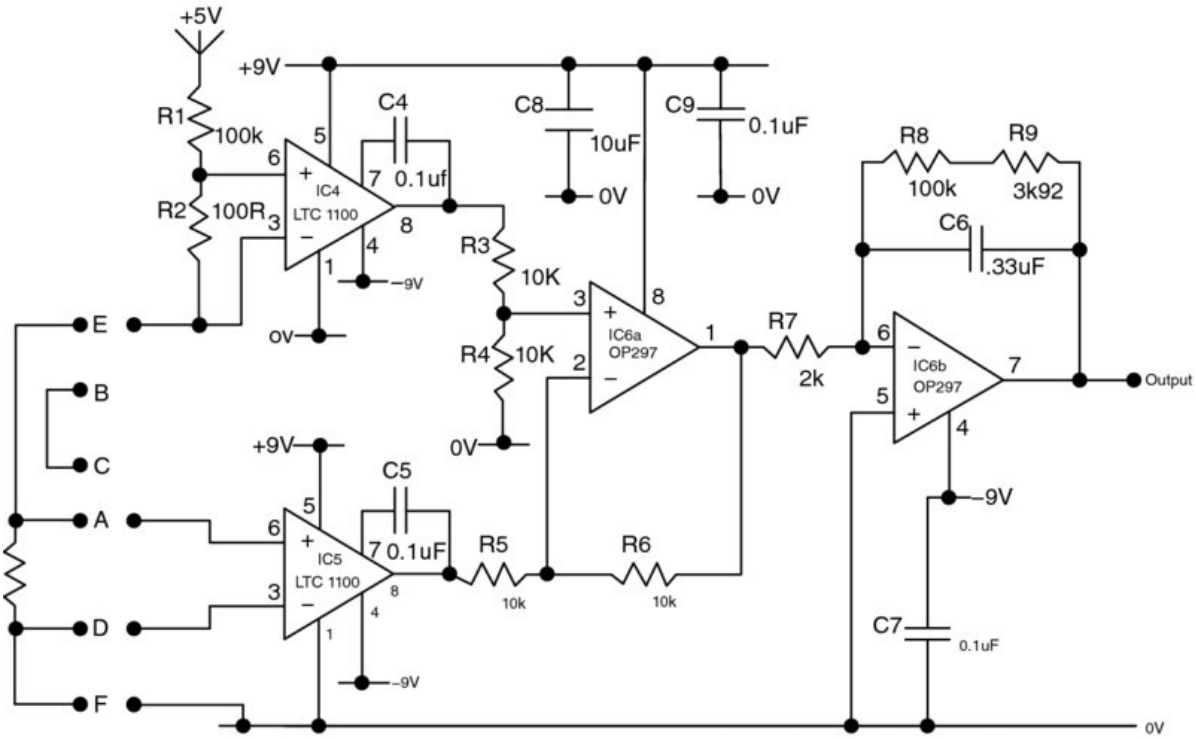

Figure 5.13 Measurement circuit for a platinum resistance thermometer, which allows for connection resistances to a sensing element of resistance *R*. The resistance element provides four connections A, E, D and F, with one pair (E and F) providing the excitation current, and the other pair (A and D), access for a voltage measurement (B and C provide a shorting link for use with alternative resistance compensation circuitry.). R1 and R2 are precision resistors, chosen for temperature stability and close tolerance.

5.5 Thermometer exposure

Solar radiation falling on a thermometer used for air temperature measurements will cause its temperature to be greater than true air temperature, causing a *radiation error*. Even for the fine wire sensors of Figure 5.10, a frame and body of non-negligible area are still required to support the fine wire element. The radiation error presents a fundamental problem for accurate air temperature measurements.

5.5.1 Radiation error of air temperature sensors

For a thermometer in thermal equilibrium with its surroundings (when its temperature is stable), the radiant energy received by the thermometer balances that lost by thermal radiation and convection, that is, when

Rate of acquisition of energy	=	Heat loss rate by radiation	+	Heat loss rate by convection

In principle, the energy received can be calculated if the geometry of the sensor is known, as this determines both the effective areas for interception of the solar radiation and for convective and radiative losses.

Consider a temperature sensor exposing an area A to radiation, constructed of material with reflection coefficient α and emissivity #. If there is no conduction away from the device, then, for an incident irradiance S, the rate of acquisition of energy is $S\,(1-\alpha)\,A$. Balancing this source term with terms for the heat loss rate by radiation and convection gives

$$S(1-\alpha)A = \varepsilon A'\sigma(T^4 - T_a^4) + \frac{k(T-T_a)}{d}A'N\,, \tag{5.9}$$

where the first RHS term represents radiative loss (from the Stefan-Boltzmann Law, with σ the Stefan–Boltzmann constant) and the second, the convective loss. Both the radiative and convective losses are assumed to occur from the same area A', which, in general, will differ from the area able to intercept the radiation A. The convective loss is found from the difference in temperature between the sensor temperature T and air temperature T_a and thermal conductivity of air, for which the constant of proportionality – the convective heat transfer coefficient – is known as the Nusselt number. The Nusselt number N is given by $N = c(\mathrm{Re})^{\zeta}$, where c and ζ depend on geometry, and Re is the Reynolds number. Re is calculated as Ud/v where U is the air speed past the sensor, d the sensor diameter and v is the kinematic viscosity of air. For a cylinder, $c = 0.62$ and $\zeta = 0.5$. Substituting for the Nusselt number gives

$$S(1-\alpha)A = \varepsilon A'\sigma(T^4 - T_a^4) + \frac{k(T-T_a)}{d}A'c\sqrt{\frac{Ud}{v}}\,. \tag{5.10}$$

Of the two loss terms on the right-hand side, the heat loss by thermal radiation is much smaller, and can be neglected in comparison. Hence the difference in temperature between the air and the sensor – this is the radiation error ΔT – is, for $A = A'$,

$$\Delta T = (T - T_a) = \frac{S(1-\alpha)d}{kN} = S\frac{(1-\alpha)\sqrt{\nu}}{kc}\sqrt{\frac{d}{U}}, \tag{5.11}$$

or,

$$\Delta T \propto S\sqrt{\frac{d}{U}}. \tag{5.12}$$

This shows that the radiation error depends directly on the amount of non-reflected radiation, but is also proportional to the sensor diameter (as $d^{1}/_{2}$ for a cylinder), and inversely proportional to the wind speed (as $U^{1}/_{2}$ for a cylinder). Laboratory experiments (Figure 5.14) using a pair of cylindrical sensors exposed to a radiation from a bright lamp under varying ventilation (Figure 5.15), confirm the form of Equation 5.12.

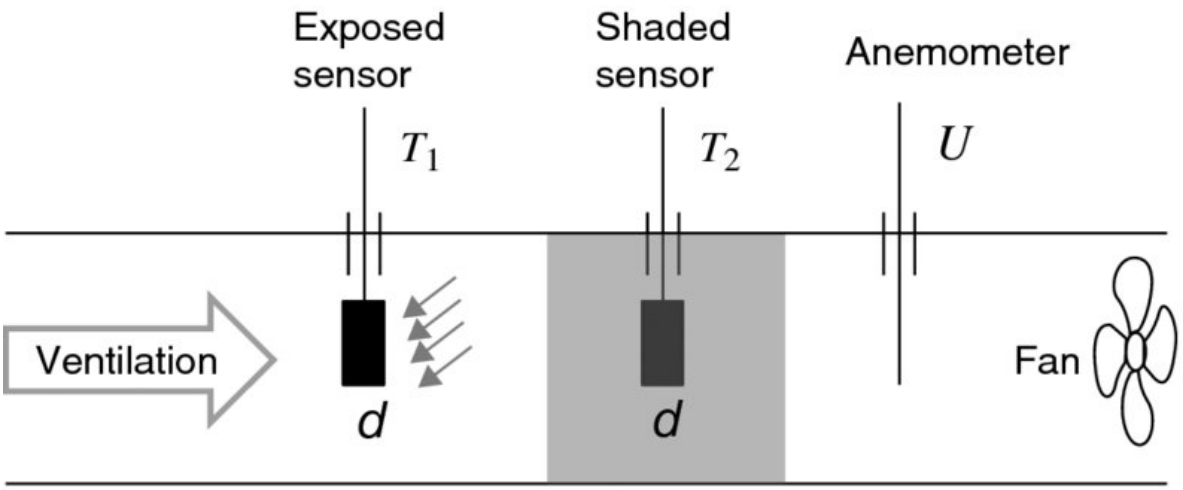

Figure 5.14 Experiment to compare the effect of radiation on two identical cylindrical sensors of diameter d, one (T_1) exposed to radiation, and the other (T_2) shaded, in ventilation of variable speed U.

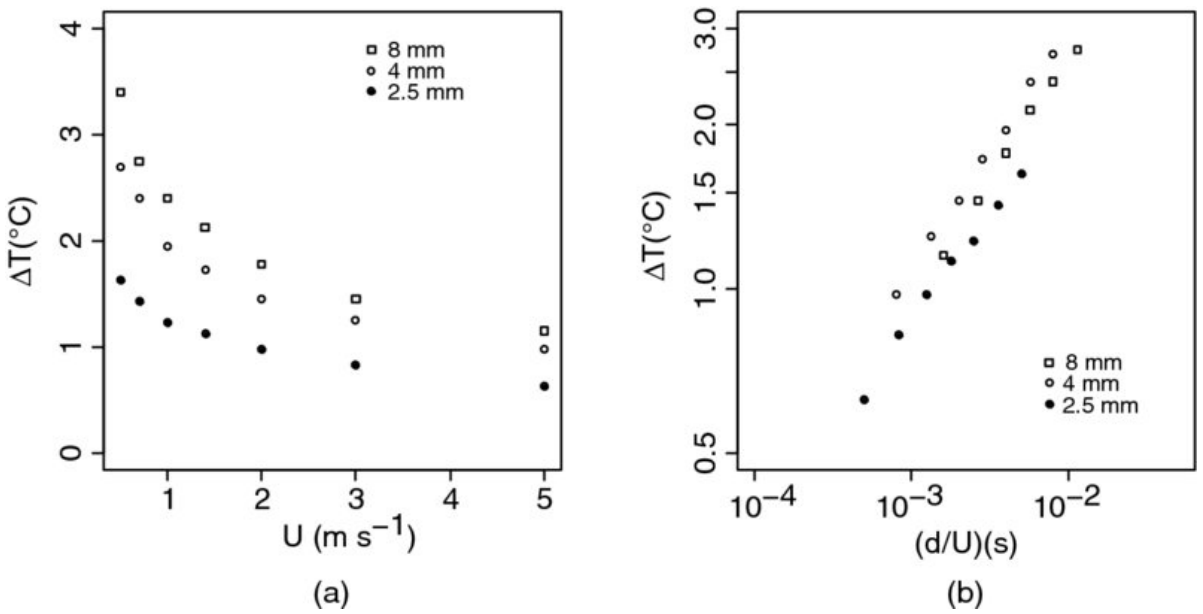

Figure 5.15 (a) Difference in temperature (ΔT) between a pair of identical blackened cylinders, one shaded and the other exposed to radiation from a 700 W tungsten lamp, with the air speed U across the cylinders varied. The experiment was repeated for pairs of sensors having diameters 2.5 mm, 4 mm, and 8 mm. (b) data from (a) plotted on a log–log plot, as (d/U) versus ΔT. (For the 8 mm diameter sensor, $\zeta = 0.46$, using a least-squares fit.)

These laboratory experiments show that, without ventilation, sensors with appreciable areas for interception of solar radiation in the atmosphere may readily record temperatures which are several degrees greater than the local air temperature.

5.5.2 Thermometer radiation screens

To minimise radiation errors in the measurement of air temperature for long-term climatology purposes, it has long been recognised (see Section 1.4) that an instrument shelter or radiation screen of some form is needed to protect the thermometer's sensing element from direct solar radiation. The basic requirements for an ideal thermometer shelter [46] are that it should:

1. provide shielding from direct rays of the sun at all times;
2. not affect the thermometers by warming up;
3. prevent reflected radiation from reaching the thermometers;
4. exclude external sources of heat (e.g. from buildings);
5. allow free passage of air around the thermometers.

Instrument shelters can of course also offer protection from precipitation for thermometers and other sensors, such as those required typically for humidity measurements.

Some hand-held instruments are specially designed to minimise radiation errors in temperature measurements, by forcing ventilation through a highly reflective housing (e.g. the Assmann psychrometer, Section 6.3.7), or by minimising the radiation interception area, for example through the use of a fine wire thermometer.

The double-louvered wooden screen of Thomas Stevenson is a well-established design of thermometer shelter, with a long and widespread legacy because few changes have been made to the original design across a century. Stevenson screens are still widely deployed at standardised measurement sites (Figure 5.16). The question of the absolute accuracy of the air temperature measurements obtained using such a thermometer screen is difficult, as it clearly requires a reference measurement of air temperature for comparison, and there are competing uncertainties in the comparison experiments required. The lag and radiation errors are generally the most important.

Figure 5.16 Stevenson screens in use at Eskdalemuir Observatory, Dumfriesshire.

5.5.3 Radiation errors on screen temperatures

In poorly ventilated conditions, radiation errors can limit the accuracy of air temperature measurements using radiation screens [47], notably in calm and/or sunny conditions. This means that the screen temperature T_{scrn} and the air temperature T_{air} may differ and hence that they cannot always be assumed to be equivalent. An extensive investigation [48] of the properties of a Stevenson screen was undertaken between October 1969 and December 1972 at Kew Observatory, London. This work used an aspirated resistance thermometer as the reference measurement most accurately approximating the true air temperature, 10 m away from the screen. This aspirated thermometer was still subject to small effects from surface reflection of solar radiation, but this was estimated to only contribute a maximum error of +0.1°C to the determination of the air temperature.

In daytime conditions, the differences between the screen temperature (T_{scrn}) and aspirated reference thermometer (T_{asp}) in the Kew experiments exceeded 1°C in winter and 2°C in summer; the mean differences obtained are summarised in Table 5.3. The largest differences found were in September when there were frequent light winds, with the worst case error in the most unfavourable conditions estimated to be 2.5°C. Occasional negative temperature differences were originally thought to be due to evaporative cooling, but full calculations showed this was insufficient to explain the values observed. The absence of an evaporative cooling effect has subsequently been corroborated [49].

Table 5.3 Differences between Stevenson screen and aspirated thermometer reference temperature ($T_{scrn} - T_{asp}$) for the maximum and minimum temperatures [48], by month

Month	$\boldsymbol{T_{scrn} - T_{asp}}$ **for maximum temperature (°C)**	$\boldsymbol{T_{scrn} - T_{asp}}$ **for maximum temperature (°C)**
January	0.04	0.11
February	0.16	0.18
March	0.17	0.14
April	0.14	0.15
May	0.28	0.25
June	0.24	0.19
July	0.34	0.21
August	0.28	0.25
September	0.41	0.32
October	0.21	0.15
November	0.01	0.08
December	0.03	0.08

During nocturnal measurements, it was found that the screen thermometer temperatures exceeded the aspirated thermometer temperatures (T_{asp}), particularly at low wind speeds (Figure 5.17). In this study, these effects were attributed to the slower response of the Stevenson screen (estimated as ∼20 min) compared with the aspirated thermometer (response time ∼2 min), in adapting to decreasing temperatures.

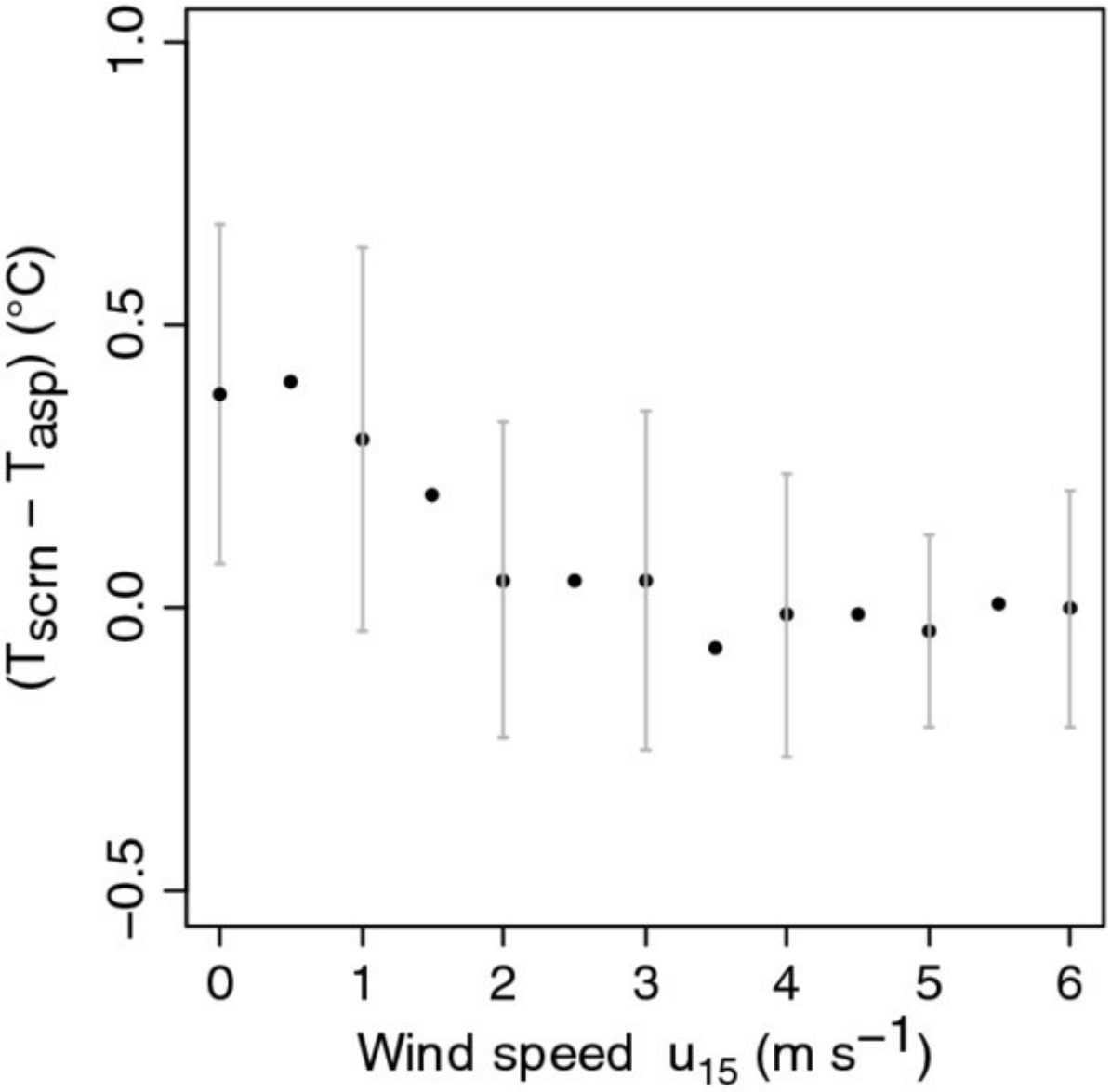

Figure 5.17 Mean differences [48] in daily minimum temperature between the temperature measured within a large thermometer screen (T_{scrn}) temperature and an aspirated thermometer's temperature (T_{asp}), plotted against wind speed at 15 m. (Standard deviations are shown using error bars, when available.)

Further insight into the behaviour of a thermometer screen, particularly under low wind speed conditions, can be obtained from comparison of the continuous variation in screen temperature with a more rapidly responding air temperature reference measurement than that available for the Kew study. A fine wire thermometer provides a useful rapid response reference thermometer in open air, but, for accurate air temperature measurements, it must also be screened from direct solar radiation. This can be achieved using a mechanical solar tracker, a device designed to track the sun for solar radiation measurements (see Section 9.4), to keep the thermometer within the shade. Figure 5.18 shows the experimental arrangement used [50]. The fine wire thermometer

was regularly compared with the thermometer with the screen to correct for any drift during its exposure.

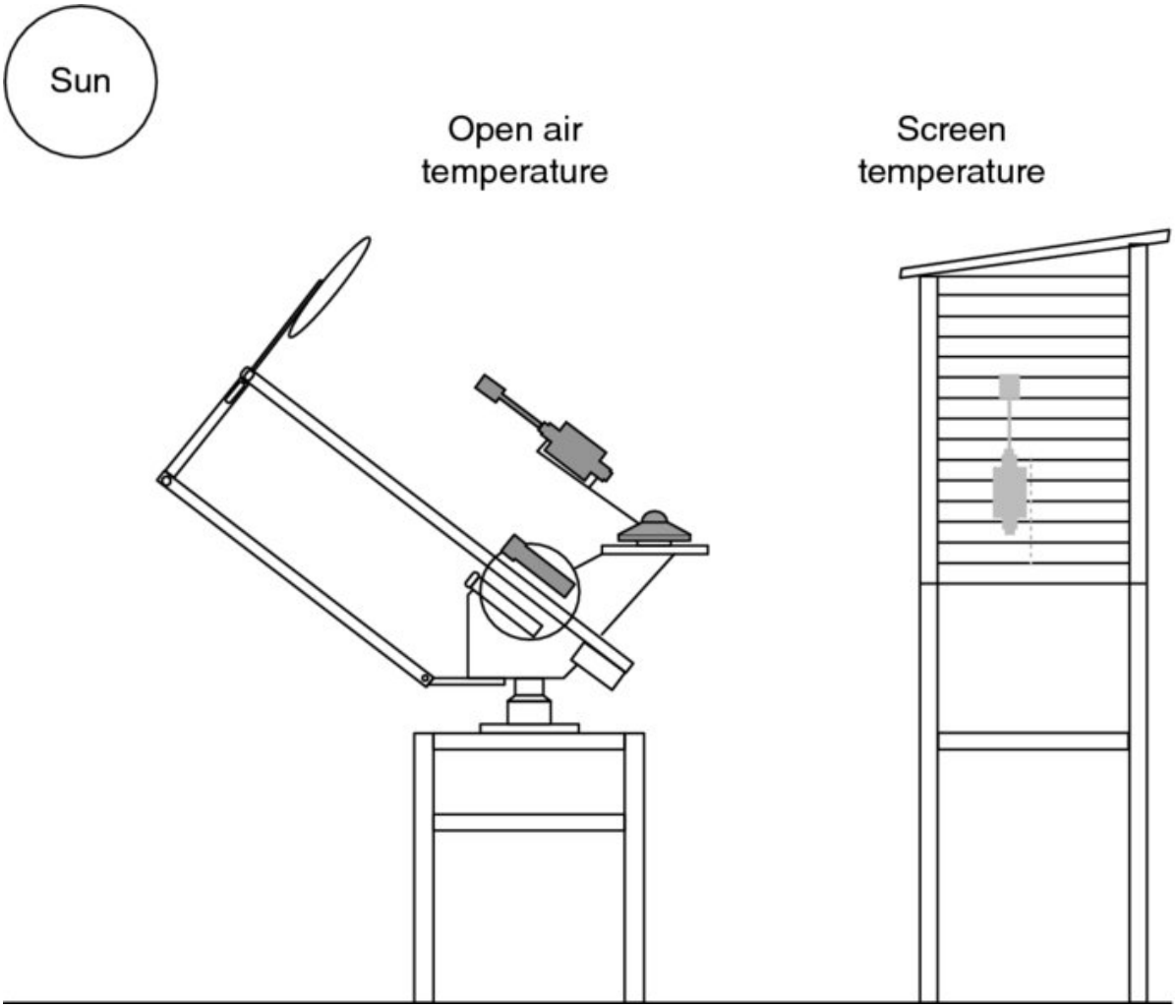

Figure 5.18 Experimental arrangement at Reading Observatory for comparing temperatures determined by a fine wire thermometer in the open air with those determined within a thermometer screen. The open air thermometer (left) is mounted on a mechanical solar tracker, which moves an occultation disk so as to keep the thermometer continuously shaded.

Measurements of the open air temperature (T_{open}) and the screen temperature (T_{scrn}) obtained during these experiments are shown in Figure 5.19, during fluctuating cloud conditions. The measurements include the solar radiation as determined on a horizontal surface, and the wind speed at 2 m above the surface, near to the thermometer screen. The difference $T_{scrn} - T_{open}$ is also shown. It is clear that this difference is variable, but that it is at its greatest under calm or low wind speed conditions as found in the Kew study. Instantaneously, the difference between the differently-exposed sensors can be over ±1°C, but the median difference is <0.2°C.

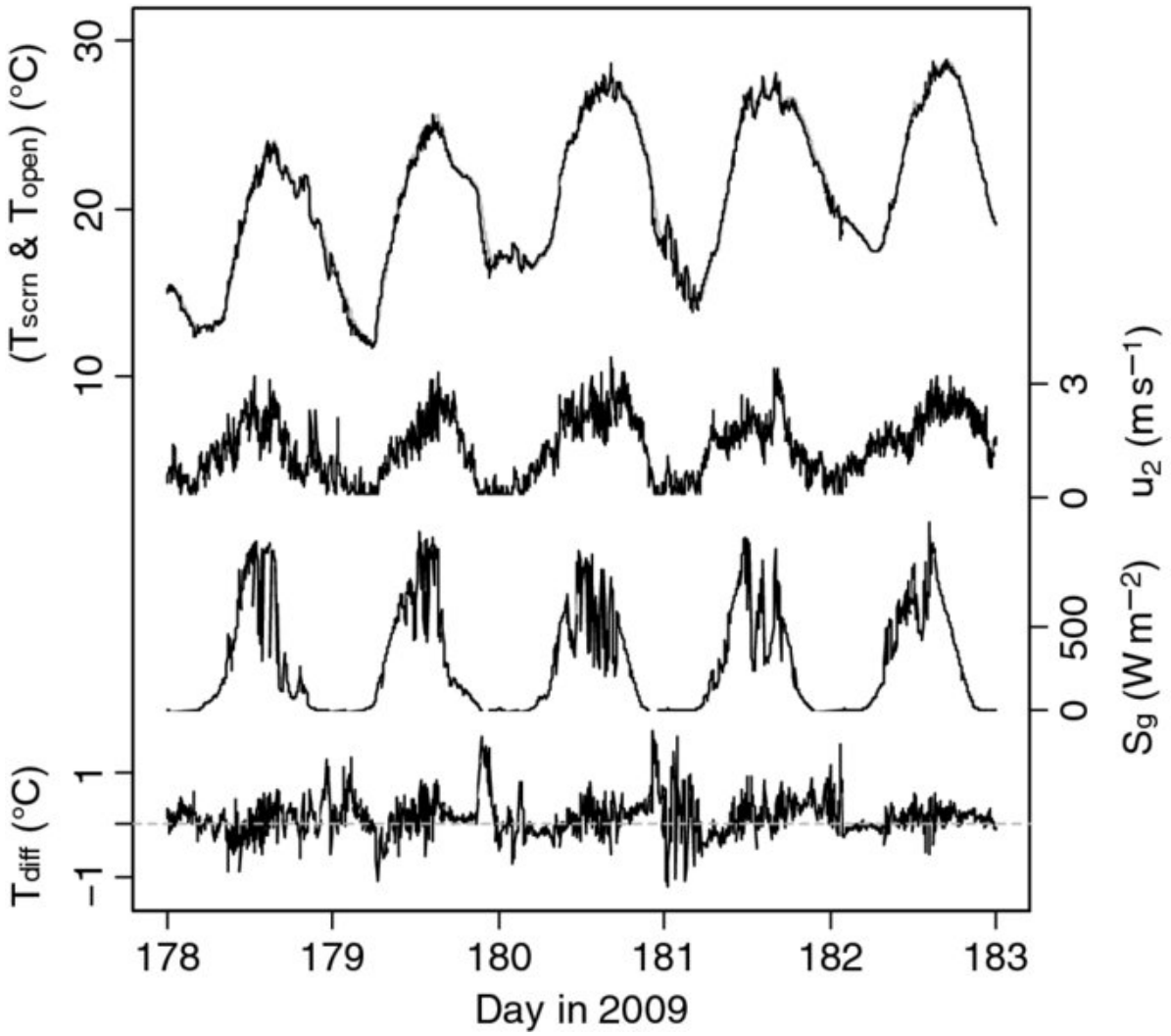

Figure 5.19 Investigation of thermometer screen response in cloudy conditions. Time series (plotted as day of year) showing (upper trace) screen temperature (T_{scrn}, thick grey line) and fine wire thermometer open air temperature (T_{open}, thin line), (second trace) 2 metre wind speed (u_2), (third trace) global solar irradiance (S_g), and (lower trace) screen-air temperature difference ($T_{diff} = T_{scrn} - T_{open}$).

On the basis of the Kew study and others, the World Meteorological Organisation [51] indicates the worst case difference between true air temperature T_{air} and screen temperature T_{scrn} in calm and clear conditions can lie between −0.5°C and 2.5°C.

5.5.4 Lag times in screen temperatures

Because of the enclosure around them, the response time of the combined screen and thermometer system is fairly slow. The lag time τ (minutes) for a thermometer screen can be represented by an expression of the form

$$\tau = \frac{A}{U^n}, \tag{5.13}$$

where U is in m s^{-1}. A = 8.2 and $n = {}^1/_2$ have been reported for a Stevenson screen [52] in wind tunnel experiments, suggesting τ is typically between 5 and 30 min. The screen's lag can also be found from a comparison of the times at which the daily maxima and minima occur in screen temperature with a separate measurement of temperature which is unscreened. Figure 5.20a shows the differences in lag time obtained using this approach for a large thermometer screen, plotted against the wind speed at 2 m obtained nearby using the experimental arrangement of Figure 5.18. The lag time increases substantially at low wind speeds (u_2 < 1 m s^{-1}), and the results are reasonably well represented by a power law fit of the form of Equation 5.13. In terms of the temperature variations, at low wind speeds, the lag time leads to a very slight reduction of the amplitude of the daily temperature cycle (Figure 5.20b). This is expected from Equation 2.7, hence the reduction of the amplitude would be greater for more rapid temperature fluctuations, such as that arising from temperature changes generated by the passage of fronts.

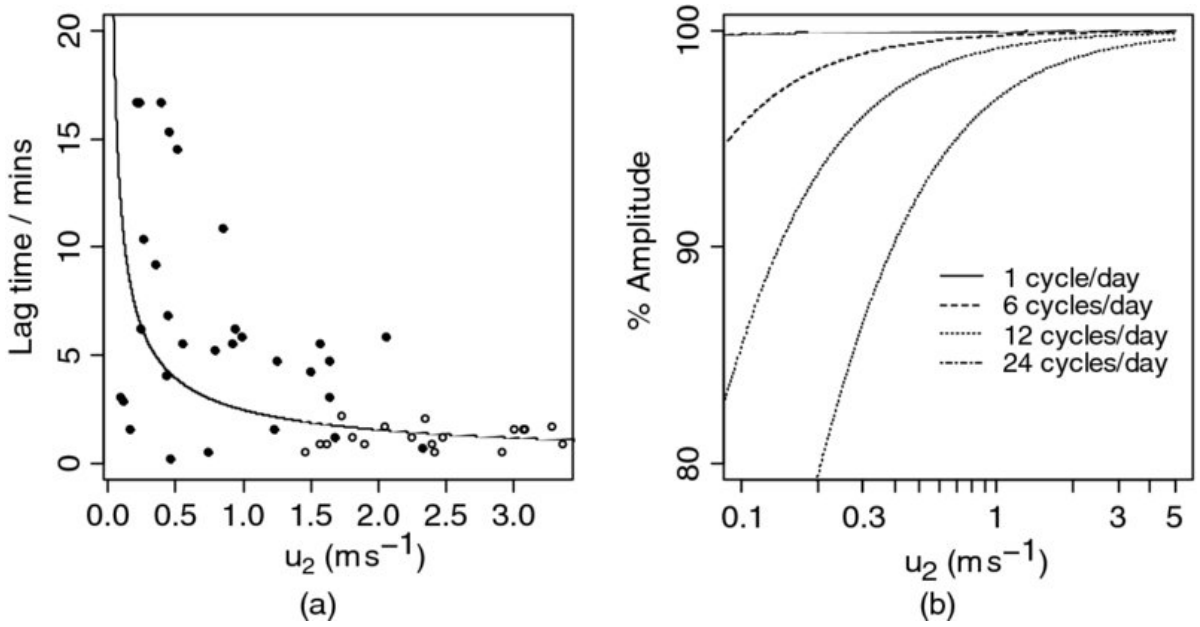

Figure 5.20 Results of a screen thermometer lag experiment [53] at Reading, 2009–2010. (a) Lag time between screen temperatures and an unscreened fine wire temperature, for minimum (solid points) and maximum (hollow points) temperatures, as a function of wind speed u_2, averaged for the hour centred on the screen temperature maximum or minimum. A power law ($\tau = 2.5\, u^{-0.7}$, for u in m s^{-1} and τ in minutes) has been fitted by regression. (b) First order amplitude reduction with wind speed for a range of sinusoidal temperature variations, using the same power law.

To compare the temperature changes which can occur with the screen response, a sequence of air temperatures measured using cylindrical platinum resistance thermometer sensors is shown in Figure 5.21. This demonstrates a fairly rapid change in air temperature, with a temperature change of over 4°C in 30 min, together with the surface wind speed providing the ventilation of the screen. In this case, comparison with Figure 5.20 shows that lag time is much shorter than the timescale of the temperature change.

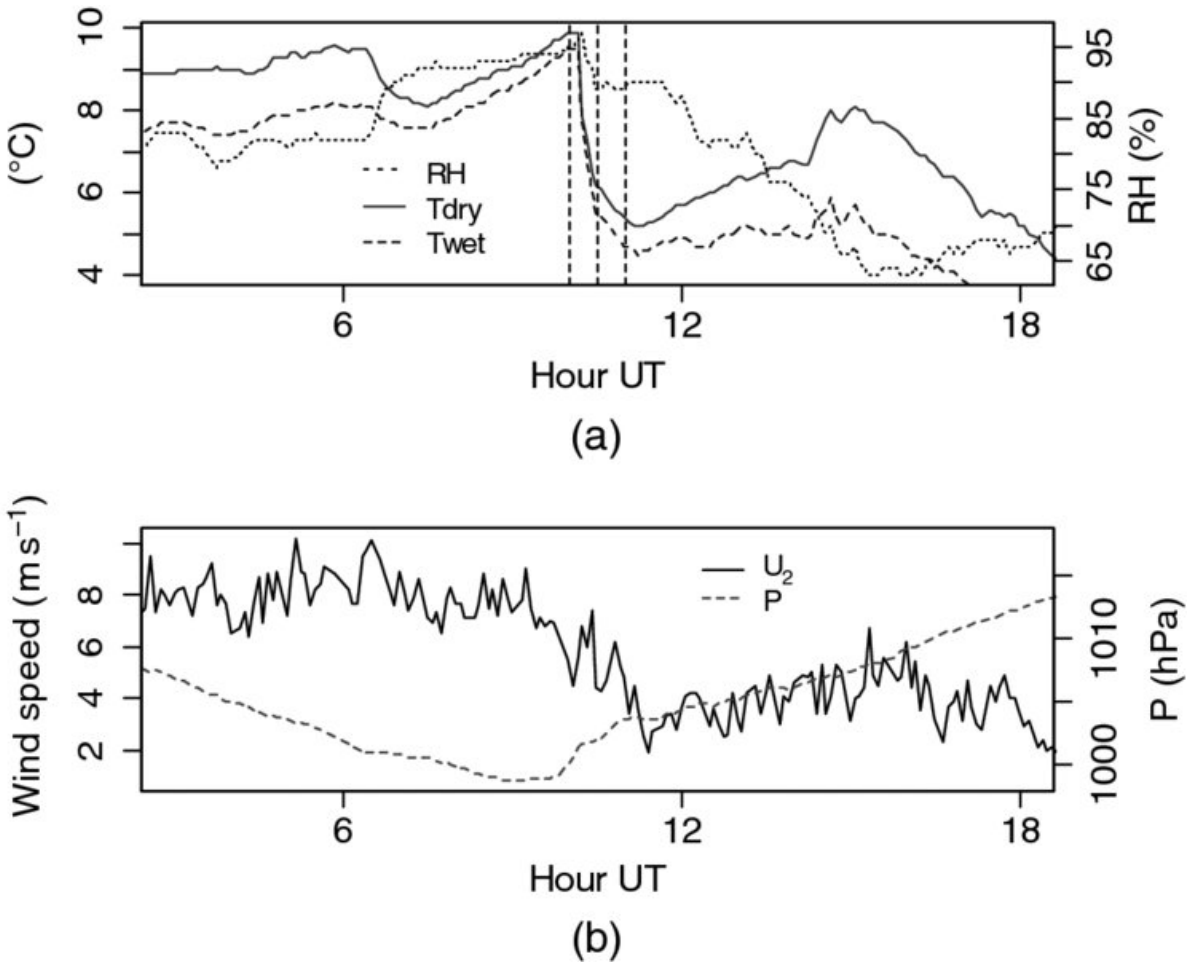

Figure 5.21 Meteorological quantities measured at Reading Observatory as 5 minute mean values, on 10 February 2000, showing air temperature (T_{dry}) in (a), together with wet bulb temperature (T_{wet}), derived Relative Humidity (RH) and (b) wind speed at 2 metres (u_2) and station pressure (P). In (a), the vertical dashed lines mark 1000, 1030 and 1100 UT.

5.5.5 Screen condition

The condition of a thermometer screen, most notably the state of the paintwork for wooden screens, is another factor influencing the temperatures observed [54]. This has been studied by comparing one small and two large screens, with an aspirated screen for the reference temperature [49]. One of the large screens was in perfect condition, and the other poorly maintained. The

study lasted 207 days, sampling the sensors 12 times per minute to form 1-minute averages (Table 5.4). The screens were all at 1.5 m above the surface within the same enclosure at Norrkoping, Sweden.

Table 5.4 Largest negative and positive temperature differences between screen and reference ($T_{scrn} - T_{ref}$), for screens in different conditions [49]

Screen compared with reference temperature	**Positive difference (° C)**	**Negative difference (° C)**
Small screen	2.62	−1.66
Large screen (good condition)	3.10	−1.68
Large screen (poor condition)	3.61	−2.06

The poorly-maintained screen produced the largest deviations, with the small screen having smallest positive and negative extremes, probably due to its more rapid response time and smaller heat capacity. The condition of the screen is therefore another important factor, and wooden screens vary considerably in the maintenance they receive, for example in the state of their paintwork of the upper reflective surface and south-facing louvres (Figure 5.22).

Figure 5.22 Thermometer screen used for climatological observations at a seaside resort.

5.5.6 Modern developments in screens

For automatic temperature recording systems using data loggers, a wide range of smaller radiation screens of different designs has emerged, generally based on the multi-plate or beehive screen (Figure 5.23). Ventilation is recommended at ~ 3 m s^{-1}, as long as moisture is not introduced [51]. Plastic Stevenson-style thermometer screens have also been produced, which require greatly reduced levels of maintenance compared with traditional wooden screens. Temperatures obtained in a plastic screen agree to better than 0.25°C with the temperatures obtained in an adjacent wooden screen: the agreement is further improved if the interior of the plastic screen is blackened [55]. Plate or beehive screens are also suitable for locations with limited space, such as on ocean buoys, on which only small thermometer screens can be fitted. Uncorrected, radiation effects on buoy temperature measurements [56] have shown a mean daytime temperature error of 0.27°C, up to a maximum error of 3.4°C.

Figure 5.23 Beehive thermometer screen in use at the meteorological site of the Universitat de les Illes Balears, Palma.

5.6 Surface and below-surface temperature measurements

5.6.1 Surface temperatures

Surface temperature measurements can be obtained from liquid-in-glass or platinum resistance sensors lying on grass, soil, tarmac, concrete or snow surfaces, as needed (see also Figure 5.7). The range of temperatures encountered for such a surface directly heated by solar radiation is, in general, much greater than the corresponding air temperature. Figure 5.24 compares air, soil, grass and concrete temperatures, showing that the greatest surface temperatures exceed the air temperatures by at least 10°C.

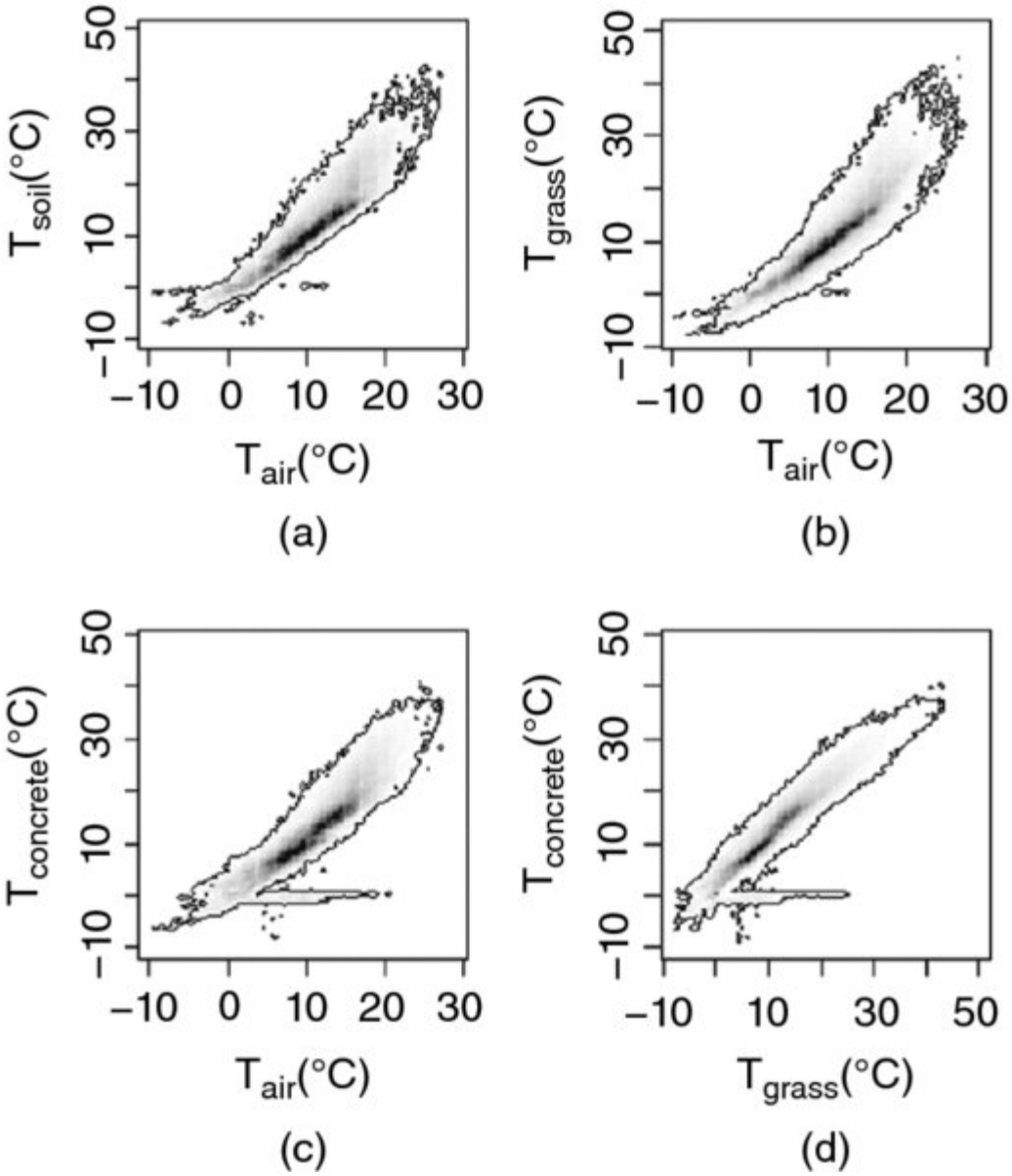

Figure 5.24 Temperatures of (a) soil, (b) grass and (c) concrete surfaces, against air temperature, measured at Reading Observatory between 2007 and 2012. (d) shows the relationship between the grass and concrete surface temperatures. (Plots show increasing density of values in increasingly darker grey tones; the outline contour shows the extreme values.)

5.6.2 Soil temperatures

Beneath the surface, soil temperature measurements at different depths can be obtained from a vertical array of temperature sensors. Figure 5.25 shows measurements made on a cloudless day using a set of thermistors fitted in a soil temperature probe pushed into the soil. Each thermistor was connected to resistance measuring apparatus using a long multi-core cable. The diurnal

variation in temperature at the surface becomes suppressed with increasing depth in the soil, and the maximum temperature value occurs later. (The soil temperature's relationship to the vertical heat flux in the soil is discussed further in Section 12.1.3.)

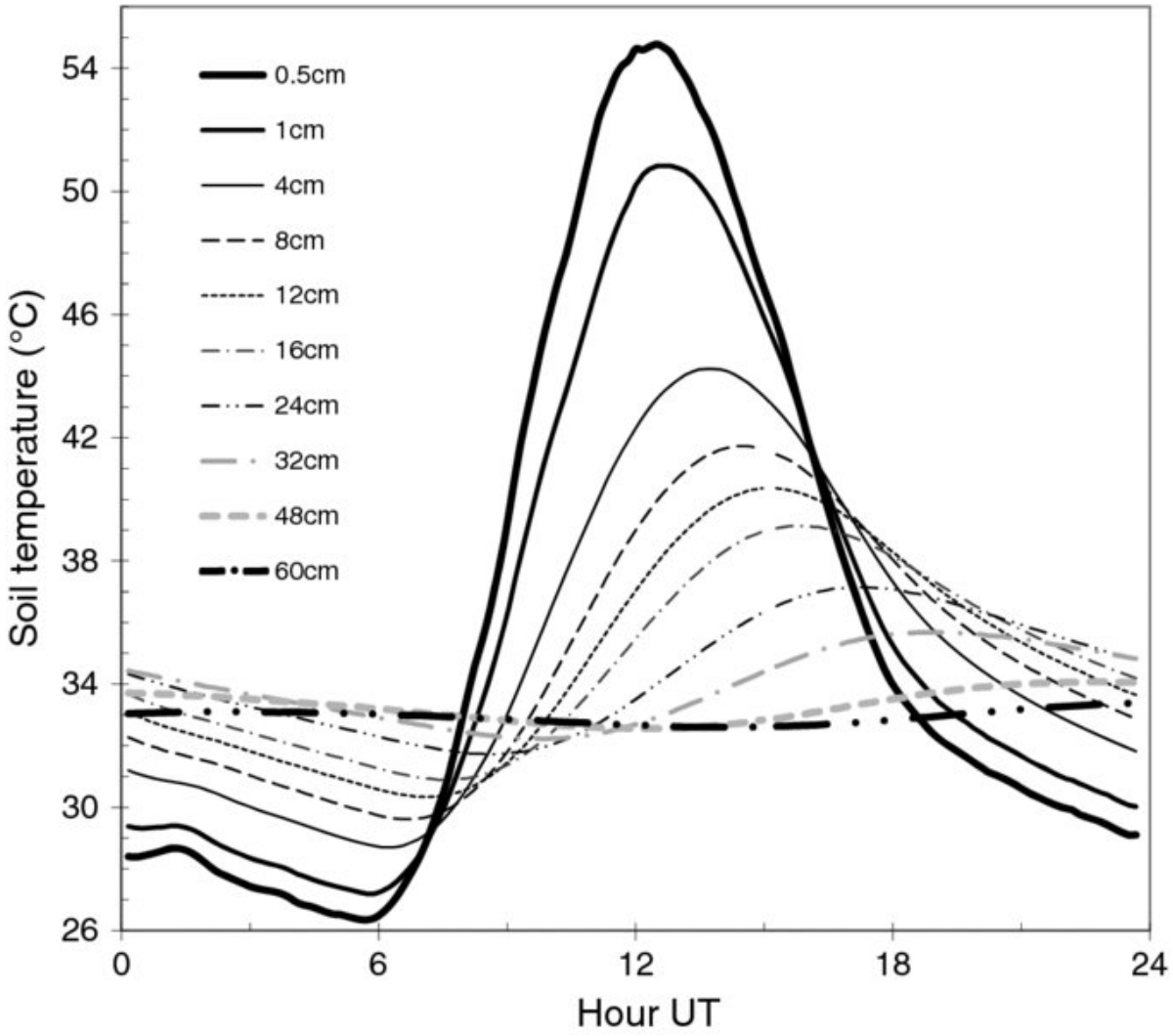

Figure 5.25 Diurnal variation of soil temperatures with depth, obtained during a cloudless day in the Sahel region of Africa (25 September 1992). The temperatures were measured as 10-minute average values, using a set of calibrated bead thermistors, vertically spaced on a wooden probe driven into the soil with the thermistor resistances measured remotely using a multi-core cable and a data logger (see also Figure 9.29).

5.6.3 Ground heat flux density

The rate of vertical transfer of heat – known as the ground heat flux density – is usually determined using a temperature measurement approach, by finding the temperature difference across a material of known thermal conductivity. Such a device is a *heat flux plate* (Figure 5.26). These are circular or rectangular devices, typically with dimensions of a few centimetres.

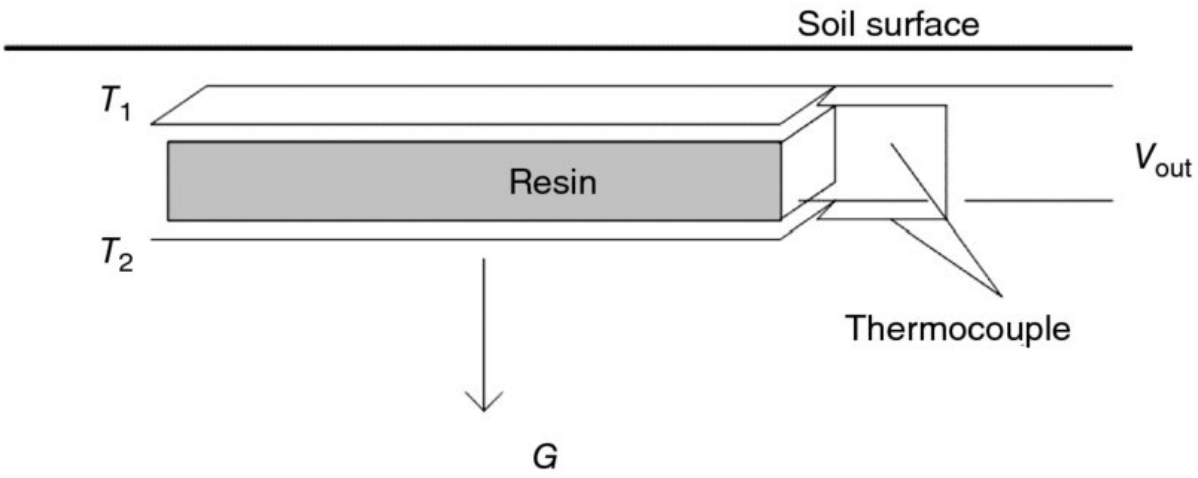

Figure 5.26 Principle of a soil heat flux plate, which determines the vertical heat flux density G by the temperature difference caused by the heat flow through a layer of resin of known conductivity.

A heat flux plate consists of two aluminium plates, sandwiching a resin of known thermal conductivity. By using a thermocouple to determine the temperature difference ($T_1 - T_2$) between the upper and lower surfaces, the heat flux can be determined by Fourier's Law. The thermocouple output voltage is sufficiently small that it will often require amplification. The thermocouple voltage is found to be directly proportional to G, and can be calibrated by applying known heat fluxes in thermal equilibrium. Uncertainties in the data from ground heat flux plates arise because their presence disturbs the heat and gas flow in a soil. There may also be poor thermal contact, and differences between the resin's thermal properties conductivity and that of soil.

Notes

1 This is the unique temperature at which the vapour, liquid and solid phases of water co-exist in equilibrium. This temperature is conveniently obtained through the use of a triple point cell, which is a cooled cylindrical glass jacket containing melting ice. A thermometer is inserted and read when solid, liquid and vapour are simultaneously present.

2 Because of the possibility that small quantities of pure water can remain liquid well below the freezing point of bulk water (i.e. through supercooling, see Figure 5.6), the melting point of ice is chosen as less ambiguous.

3 Minimum or maximum thermometers exist based on LiG thermometers, which retain the extreme value of temperature reached until it is reset. In modern variants of the combined

maximum and minimum thermometer originally designed by James Six (1731--1793) in 1782, the extreme temperatures reached are marked by a metal index moved by the mercury column, which can be reset using a magnet.

4 Generating a thermocouple emf is an example of the *Seebeck effect*. If, instead, a current is applied, one junction will cool with respect to the other, which is known as the *Peltier effect*. Qualitatively, both effects are associated with a thermal gradient across the metal junction, causing charge carriers at the hot end of a metal to have more energy than those at the cold end, with the excess energy exchanged with the metal lattice.

5 A negative temperature coefficient device has a response in its thermometric property (resistance in the case of a thermistor) which decreases with increasing temperature.

6 This is a simplified form of the Callendar–Van Dusen equation for platinum resistance thermometry, which arose from the work of the Gloucestershire-born physicist Hugh Longbourne Callendar (1863–1930). His son, Guy Stewart Callendar (1898–1964) pioneered the idea that rising atmospheric carbon dioxide concentrations influence the global temperature.